Published in final edited form as:
Pain. 2010 July ; 150(1): 93–102. doi:10.1016/j.pain.2010.04.001.

Temporal summation of heat pain in humans: Evidence supporting thalamocortical modulation

Tuan D. Tran[1,2,3], **Heng Wang**[1,2], **Animesh Tandon**[4], **Luis Hernandez-Garica**[5], and **Kenneth L. Casey**[1,2,*]

[1]Department of Neurology, University of Michigan, Ann Arbor, MI 48109, USA

[2]Neurology Research Laboratory, VA Medical Center, Ann Arbor, MI 48105, USA

[3]Department of Pediatrics, University of Medicine and Pharmacy of Ho Chi Minh City, Ho Chi Minh City, Vietnam

[4]Medical School, University of Michigan, Ann Arbor, MI 48105, USA

[5]Department of Biomedical Engineering and Functional MRI laboratory, University of Michigan, Ann Arbor, MI 48109, USA

Abstract

Noxious cutaneous contact heat stimuli (48°C) are perceived as increasingly painful when the stimulus duration is extended from 5 to 10 seconds, reflecting the temporal summation of central neuronal activity mediating heat pain. However, the sensation of increasing heat pain disappears, reaching a plateau as stimulus duration increases from 10 to 20 seconds. We used functional magnetic resonance imaging (fMRI) in 10 healthy subjects to determine if active central mechanisms could contribute to this psychophysical plateau. During heat pain durations ranging from 5 to 20 s, activation intensities in the bilateral orbitofrontal cortices and the activation volume in the left primary (S1) somatosensory cortex correlated only with perceived stimulus intensity and not with stimulus duration. Activation volumes increased with both stimulus duration and perceived intensity in the left lateral thalamus, posterior insula, inferior parietal cortex, and hippocampus. In contrast, during the psychophysical plateau, both the intensity and volume of thalamic and cortical activations in the right medial thalamus, right posterior insula, and left secondary (S2) somatosensory cortex continued to increase with stimulus duration but not with perceived stimulus intensity. Activation volumes in the left medial and right lateral thalamus, and the bilateral mid-anterior cingulate, left orbitofrontal, and right S2 cortices also increased only with stimulus duration. The increased activity of specific thalamic and cortical structures as stimulus duration, but not perceived intensity, increases is consistent with the recruitment of a thalamocortical mechanism that participates in the modulation of pain-related cortical responses and the temporal summation of heat pain.

[*]**Corresponding author:** Department of Neurology University of Michigan Ann Arbor, Michigan 48109 U.S.A. kencasey@umich.edu voice mail: 734-971-4207 fax: 734-971-7915 .

1.INTRODUCTION

Noxious heat activates low threshold (~40°C) and high threshold (> 46°C) heat receptors innervated by slowly conducting (~1.0 m/s) unmyelinated C fibers and by the faster conducting (~15 m/s) finely myelinated A fibers. The temporal and spatial integration of postsynaptic potentials generated by these nociceptive afferent fibers leads to the temporal recruitment of second order central neurons and the subsequent activation of brain mechanisms mediating pain. Functional imaging studies show that brain activation changes during a prolonged, repetitive, cutaneous application of a painfully hot probe. For example, a positron emission tomographic (PET) activation study revealed that, during the first 60 s of repetitive noxious contact (5 s) heat stimulation, activity appears first in frontal structures such as the premotor, anterior cingulate, prefrontal, and anterior insular cortices. Later, following an additional 40 s of repetitive stimulation, activity appears in the secondary (S2) somatosensory and mid-insular cortices and in the contralateral primary sensori-motor cortex, ventral posterior and medial thalamus, and in the cerebellum; these activation changes are accompanied by increases in the perceived intensity and unpleasantness of the heat pain [11].

Applying noxious contact heat to the skin continuously, rather than repetitively, reveals a modulation of perceived heat pain and temporal summation. As the duration of a constant noxious heat stimulus increases, the perceived intensity of heat rapidly increases above heat pain threshold when the stimulus duration is extended from 5 to 10 s. However, as the duration of the noxious heat stimulus increases beyond 10s to 30 s, the perceived temporal summation ceases and the perceived intensity remains nearly constant during this period [21,34]. This result suggests that, at some time near 10 s after stimulus onset, peripheral or central mechanisms, or some combination of the two, begin to limit perceived pain intensity to create what we will refer to here as a *psychophysical plateau*. Koyama and colleagues [34] suggested that the psychophysical plateau could be accounted for either by an early burst of activity followed by a later sustained lower rate of discharge in A and C heat nociceptive afferents [13,4,10,67,66], or by central mechanisms suppressing the heat pain modulatory effects of warm afferents[12,16]. To determine if thalamocortical mechanisms could also contribute to the psychophysical plateau, we used functional magnetic resonance imaging (fMRI) to examine the time course of brain activations during prolonged heat pain. We examined brain activation while noxious contact heat was applied to the skin for 5, 10, and 20 s. In accord with previous findings [11], we observed changes in brain activation as stimulus duration increased; some of these changes are consistent with the participation of thalamocortical mechanisms in modulating temporal summation and heat pain intensity.

2. Methods

2.1 Subjects

Fourteen paid healthy volunteers (7 males and 7 females, average age 25.4 ± 4.7 (mean ± SD) years) participated in this study. All fourteen subjects participated in the psychophysical experiment. Among them, ten subjects (5 males and 5 females) participated in the fMRI experiment and were 24.8 ± 4.5 (mean ± SD) years old. All subjects were right handed. They were free of medication and had not ingested any psychoactive compounds, including caffeine, within 24 hours of the day of testing. Each subject signed a consent form after receiving a complete explanation of the purpose and design of the study. The experimental protocol was conducted in accordance with the Helsinki declaration and was approved by the Internal Review Boards of the Veterans Affairs Medical Center and the University of Michigan, Ann Arbor, MI, USA. One subject whose first fMRI session revealed a cerebral malformation was excluded from further scan and analysis and was referred to the Department of Neurology at the University of Michigan for further consultation.

2.2 Heat stimulation

We applied contact heat stimuli to the hairy skin of the lateral side of both legs with a Peltier-type Thermal Sensory Analyzer device (TSA, Medoc Inc., Haifa, Israel). The area of the thermode was 16 × 16 mm^2. The baseline thermode temperature was 35°C. The ramp rate, rise and fall, was 5°C/s with feedback control. The target temperatures were 43°C and 48°C and stimulus plateau durations were 5, 10 and 20 s. A stimulus started when the probe was placed on the skin and the temperature departed from baseline; stimulation continued through the plateau phase and ended when the temperature returned to baseline. Thus, the target temperature was attained within 1.5s for the 43°C stimulation and within 2.5s for the 48°C stimulation.

2.3 Psychophysical experiment

We used 6 different stimulus conditions consisting of 2 temperatures (43°C and 48°C) and 3 plateau durations (5, 10 and 20 s). Each subject received 4 trials for each stimulus condition in each leg. A total of 48 trials were pseudorandomly given to the two legs at 48 predetermined sites. Therefore, all trials were applied on previously unstimulated sites of the skin to avoid sensitization and adaptation. The interstimulus interval (from the end of the previous stimulus to the start of the next stimulus) was 30 s and the 48 trials were divided into 4 separate runs with an approximately 2 minute break between runs. The thermode was applied on and removed from the skin 2 s before and after the stimulus.

During each stimulus presentation, subjects rated their real-time pain sensation by using their right hand to move the slider of a Computerized Visual Analog Scale device (COVAS, Medoc Inc., Haifa, Israel). The rating scale ranges from 0 to 100 with 0 = no heat sensation, 50 = heat pain threshold, and 100 = intolerable heat pain. Before the experiment, each subject received a test run applied on the inner side of the legs. The test run was similar to the ones to be delivered during the session. This practice run acquainted the subjects with the stimulation procedure, the response apparatus, and reduced the novelty effect of sensory stimulation. Subjects sat in an armchair in a quiet room with an ambient temperature of approximately 24°C throughout the experimental session. The monitor was placed in the opposite direction so that subjects could not see the stimulus and response screen.

We used a one-way ANOVA with post-hoc t-tests to compare, across the three stimulus durations, the average COVAS peaks and average areas under the COVAS curves of the 14 participants in the psychophysical experiment.

2.4 Functional magnetic resonance imaging (fMRI) experiment

2.4.1 fMRI acquisition—Ten of the 14 subjects recruited for the psychophysical study participated in the fMRI experiment; all were screened for safety and gave informed consent in accord with the University of Michigan Internal Review Board. Functional MRI experiments were carried out on a 3.0-Tesla GE Signa (Milwaukee, WI) scanner. The BOLD images were acquired continuously in each contiguous plane using single-shot, gradient-echo spiral imaging with reverse sequence only and the following parameters: echo time (TE) 28 ms, repetition time (TR) 1 s, flip-angle (FA) 70°, field of view (FOV) 24 × 24 cm, matrix 64 × 64, slice thickness 5 mm, 22 slices, no slice gap, number of excitation (NEX) 1.

Figure 1 summarizes the stimulation procedure. We obtained fMRI images using a single-epoch design [33] . There were 2 sessions corresponding to 2 different temperatures (43°C and 48°C). The 2 sessions were performed on two different days 4-7 days apart. The sequence of sessions was pseudorandomized and counter balanced across subjects. In each session (43°C or 48°C), we applied heat for three different durations with plateau phases of

5, 10 and 20 s. Each subject received 5 trials for each stimulus condition in each leg (15 stimulus trials). A total of 30 trials, divided into 5 runs with 6 trials each, were given with different stimulus durations presented pseudorandomly to the two legs at 30 predetermined sites. An epoch of each trial was 90 s. Each epoch consisted of a 30 s stimulus period between two baseline periods (30 s pre- and 30 s post-stimulus periods). Thus, each acquisition series consisted of 90 fMRI images, each run of 540 images (TR = 1s) and a total of 2700 images for each session. The interval between runs was approximately 2 minutes. We used E-Prime software (version 1, beta 5.0, Psychology Software Tools, Pittsburgh) and IFIS system (MRI devices, Waukesha, WI) to control the sequence of experiments and present messages to subjects via goggles. The E-prime computer was also used to trigger the onset of the scanner RF pulse through a TTL pulse. The experiment started with a message asking subjects to pay attention on the stimulus. The message lasted through the duration of an epoch with a 5 s interrupt asking subjects to rate the intensity of the stimulus. Subjects were not told to expect a reward for any type of response; also, they were not informed about the results of the psychophysical experiment, the intensity or duration of any stimulus in either session, or about any relationship between stimulus intensity and duration in either session. The thermode was applied 2 s before a new epoch and taken off 2 s after the stimulus period. Ten seconds after the stimulus period, a rating task message was presented on screen for 5 s asking the subject to rate the maximum intensity of the stimulus by using the right hand to press a 5-button response unit. The rating scale ranges from 0 to 5 with 0 = no warm sensation, pressing no button, 1 = warm sensation, using the thumb to press the first button, 2 = pain threshold, using the index finger to press the second button, 3 = painful, using the middle finger to press the third button, 4 = very painful, using the ring finger to press the fourth button, and 5 = intolerable pain, using the little finger to press the fifth button. The rating responses were stored for later modeling analysis.

2.4.2 Structural MRI acquisition—For anatomical reference, a high-resolution T1-weighted gradient echo image (GRE) was collected at the same prescribed location before the functional experiment (TR 200 ms; TE 3.4 ms; FA 90°; FOV 24 × 24 cm; matrix size 256 × 256; slice thickness 5 mm with no slice gap; 22 slices; NEX 2), and a high-resolution structural T1 weighted three-dimensional spoiled gradient-echo image (3D-Inversion SPGR) of the whole brain was acquired after the functional session was completed (TI 200 ms; TR 10.5 ms; TE 3.4 ms; FA 25°; FOV 24 × 24 cm; matrix 256 × 256; slice thickness 1.5 mm with no slice gap; 106 slices; NEX 1).

2.4.3 Image processing—We used the functional image analysis package FSL 3.2 for imaging processing and statistical analysis (http://www.fmrib.ox.ac.uk/fsl/) except for slice timing and motion correction. The functional data were corrected for slice timing through a *sinc interpolation* of the eight nearest neighbors in the time series and motion corrected through *AIR 3.08 Routines* [74]. The initial six scans in each run were discarded because of non-equilibrium magnetization. The functional images were spatially smoothed with 5-mm full width at half maximum (FWHM) Gaussian kernel, temporally high-pass filtered with a cutoff period of 90 s, and normalized for global signal intensity. Using a 3D affine transformation, each subject's functional images were coregistered to their GRE image with 7 degrees of freedom (DOF), and then transformed into the high resolution SPGR anatomical image with 12 degrees of freedom. The functional images were finally spatially normalized to the MNI152 (defined by Montreal Neurologic Institute) standard stereotactic space with 12 DOF. The image transformations were confirmed by visual inspection.

2.4.4 Statistical analysis of functional data—The statistical analysis was based on a least-squares estimation using a general linear modeling approach [20,19] with nonparametric local autocorrelation correction [75] to localize regions of significant

change. In all analyses, the fitting of the predictive model function with functional signal intensity was evaluated by calculating a *t* statistic on a voxel-by-voxel basis. The *t* values were then converted to *Z* scores for calculating *P* values on the basis of Gaussian random field theory [76,18]. We used the averaged COVAS time courses (6 time courses corresponding to 6 conditions) of perceived pain intensity obtained during the psychophysical experiment to derive the predictive model functions for the general linear modeling analysis. For each stimulus, the corresponding averaged COVAS time course was scaled with the rating (1-5) of the trial in the scanner, and modeled as a delta function convolved with the double gamma hemodynamic response function with its first derivative as implemented in FSL. For both within and intersubject group analyses, clusters of voxels exceeding a Z score > 2.0 and $P < 0.05$ were considered statistically significant. We used a mixed effect model for group statistics in higher level analyses. In addition to main effects we also performed contrast effect analyses among different durations.

Significant activations were calculated within pre-defined volumes of interest (VOI). The VOIs were first defined as boxes based on the atlas of Talairach and Tournoux [65]. These boxes were then converted into MNI space superimposed on the probability-estimated VOI (http://hendrix.imm.dtu.dk/services/jerne/ninf/voi.html) [49] with thresholds of $P < 0.05$ selected following visual inspection. The overlap volumes were the VOIs used in calculating significant activations. The VOIs were designed to capture structures expected to respond during pain according to the literature and included primary and secondary somatosensory cortex (S1 and S2), anterior and posterior insula (AntIns and PosIns), pregenual-, anterior-, mid-, and posterior cingulate cortex (PregCC, ACC, MidCC and PostCC), medial and lateral thalamus (MedThal and LatThal), hippocampal formation (Hipp), premotor cortex (PreMot), dorsal lateral prefrontal cortex (DLPFC), medial prefrontal cortex (MedPFC), inferior parietal lobule (InfPar), and orbitofrontal cortex (OFC) [51,70,1,9,68,[6]]. These VOIs in standard space were warped into each individual space, and voxels with significant activities that fell into these individual space VOIs were averaged for time series analysis.

We performed a one-way repeated measures ANOVA of the voxel counts and BOLD signals within each VOI across the three stimulus durations. In each case, a post-hoc Bonferroni *T* test was used for pair-wise multiple comparisons with a corrected significance level of $P < 0.05/3 = 0.017$. In addition, we analyzed the correlation (2-tailed) between the average individual voxel counts, BOLD signals, and durations, with $P < 0.01$ considered significant. We used SPSS (versions 12.0 and 15.0) software for statistical analyses.

3. Results

3.1 Psychophysics

As shown in Figure 2A, an innocuous contact heat stimulus of 43°C is not perceived as more intense as stimulus duration increases from 5 to 20 s; indeed, the average COVAS ratings show a slight decline with increasing stimulus duration. In contrast, contact heat stimuli within the noxious range (48°C) are perceived as increasingly intense, rising above heat pain threshold (COVAS 50) when the stimulus duration is extended from 5 to 10 s. For these noxious heat stimuli, there is a monotonic increase in perceived intensity that reaches a peak just before the stimulus is removed. These results simply demonstrate the well-known phenomenon of the temporal summation of perceived heat intensity above, but not below, heat pain threshold. However, as the duration of the noxious heat stimulus increases beyond 10 to 20 s, there is no perceived temporal summation. The peak perceived intensity does not increase further but remains nearly constant throughout the 20 s stimulus; this *psychophysical plateau* is shown for the average real-time COVAS ratings (Fig. 2A), the average peak COVAS ratings of each subject (Fig. 2B) and the group average COVAS ratings (Fig. 2C) of all 14 participants in the psychophysical experiment. The bar graph in

Figure 2D shows that the average peak COVAS at 5s is significantly different from that at 10 and 20s ($p < 0.001$) but does not increase between 10 and 20s ($p = 0.413$; one-way ANOVA with post-hoc 2-tailed t-tests). The duration and area under the COVAS curve (AUC) continues to increase during this period. These data are consistent with the observations of Koyama and colleagues [34] (see also [21]).

During the 43°C stimulation sessions, the 300 within-scanner post-stimulus ratings averaged 1.60 (+/− 0.694 s.d.) with a range of 1 to 4. During the 48°C sessions, the average rating was 4.31 (+/− 0.899 s.d.) with a range of 1 to 5. The difference of the means is significant ($p < 0.001$; 2-tailed 2 sample t-test).

3.2 Functional MRI

The 43°C stimuli resulted in activations only in the left dorsolateral prefrontal cortex during all stimulus durations, consistent with the lack of temporal summation of innocuous warmth in the psychophysical experiment (Figure S1, on-line supplementary material). The presence of activations or deactivations in a contrast condition can affect activations in the condition of interest. Because the purpose of this study was to investigate the temporal summation of heat pain and because of the limited and unchanging activations during the 43°C stimulation, we present here only the results of activations during the 48 °C stimulation.

During the first 5 s of 48°C stimulation, the group analysis shows active clusters in all VOI within the frontal and anterior insular cortex (Figure 3); there is no activation within the thalamus or posterior insula. The only other activation outside the frontal lobe and anterior insula at this time is in the right inferior parietal lobule (red circle in Fig. 3; MNI coordinates: 54, −44, 40). As the 48°C stimulus duration increases from 5 to 10 and 20 s, cerebral activations shift from the ACC, PregCC, AntIns, OFC, MedPFC and DLPFC to the PosIns and thalamus. The changing pattern of activation is especially pronounced as the stimulus duration is extended from 10 to 20 s. At this time the right inferior parietal activation disappears and a later activation appears in the leg area of primary somatosensory cortex (S1,blue circle in Fig. 3; MNI coordinates: −8, −38, 58). There is also an increase in the amplitude and duration of the normalized BOLD response in the right medial thalamus as stimulus duration increases as shown in the example in Fig. 3. The shift of activation shown in the main effect analysis is confirmed in the group contrast shown in Figure 4. These contrasts reveal a clear shift from the frontal cortex to the thalamus and PosIns; the later S1 cortical activation is seen also. Thus, during the psychophysical plateau of perceived intensity, activity in the thalamus and PosIns increases.

To examine further the changes in brain activation as stimulus duration increases, we performed a one-way repeated measures analysis of variance (ANOVA) on the voxel counts and peak BOLD signals in each VOI. The ANOVA and corrected post-hoc comparisons, presented in Table 1 A and B, show that both BOLD signal and voxel count increased across stimulus duration bilaterally in the LatThal, MedThal, PosIns, left S2 cortex, and the right MidCC and OFC. The bilateral MedThal, left PosIns and S2 cortex also showed both BOLD and voxel count increases specifically during the psychophysical plateau (10 vs 20 s). Significant voxel count increases appeared during this period in the bilateral LatThal, right PosIns, and right MidCC; the right OFC and left Hipp showed BOLD signal increases. These results could reflect activation changes related to either stimulus duration, perceived heat intensity, both of these variables, or to unknown co-variables.

To assess the relative contribution of stimulus duration or perceived heat pain intensity to the changes in brain activation, we performed two-tailed correlation analyses of the average peak BOLD signal and voxel count against stimulus duration and average peak COVAS rating for each subject at each stimulus duration. Structures showing a significant positive

correlation of both BOLD signal and voxel count with stimulus duration, but not with COVAS rating, would be of greatest interest because, by both of these measures, these structures would be most likely to participate in a duration-dependent modulation of perceived heat intensity and could therefore contribute to the psychophysical plateau. As shown in Table 2, the right MedThal and PosIns and the left S2 cortex (bold italicized and underlined font) possess the above characteristics; as expected, these structures also show BOLD signal and voxel increases during the psychophysical plateau (ANOVA, Table 1). No structures showed both BOLD signal and voxel count increases correlated positively and exclusively with COVAS rating. However, the left S1 cortex and the bilateral orbitofrontal cortices (LOFC, ROFC) show positive voxel count (S1) or BOLD signal (bilateral OFC) increases only with the peak COVAS rating but not with stimulus duration. The left S1 and OFC cortices also show no change in BOLD signal or voxel count during the psychophysical plateau (Table 1); the right OFC shows a BOLD signal, but not a voxel count, increase during this period. The left S1 and bilateral OFC, then, would be among the structures with activity most closely and least ambiguously associated with perceived heat pain intensity; these structures are less likely to participate in the modulation of perceived intensity during the psychophysical plateau. Figure 5 summarizes the major findings, showing the percentage changes in COVAS rating with changes in either the voxel count or BOLD signal of the above structures.

Other structures shown in Tables 1 and 2 may also mediate modulatory or sensory functions but our analyses did not identify these as clearly as those discussed above. For example, the right LatThal also shows both BOLD and voxel increases correlated only with duration but the BOLD correlation was slightly less robust ($0.01<p<0.05$) and only the voxel count showed changes during the psychophysical plateau. The activity in other structures also correlated only with duration as determined by either BOLD signal (left PregCC) or voxel count (bilateral MidCC, right S2 and ACC; left MedThal and OFC) but not by both measurements. Some structures (left LatThal, PosIns, InfPar, and Hipp) had voxel increases correlating with both COVAS rating and stimulus duration; except for the left PosIns, these structures did not show either BOLD signal or voxel count changes across duration by ANOVA analysis so it is not possible to implicate them as serving primarily either modulatory or intensity perception functions based on our analyses. Finally, we observed that the PostCC showed a slight but significant bilateral BOLD signal decrease correlated only with the peak COVAS rating, the only structure showing deactivation in this analysis. Although many of the above brain activation changes could be related to modulatory or perceptual functions, we have chosen to emphasize the most robust evidence, which implicates the left S1 cortex and bilateral OFC as mediating perceived intensity (COVAS rating) and the right MedThal, PosIns, and left S2 cortex as participating in the modulation of perceived intensity during the psychophysical plateau.

4. Discussion

Brain activations directly mediating heat intensity perception are likely to follow the time course of the perception (COVAS in this case) but those that do not follow this time course may participate additionally or exclusively in other functions, including the modulation of nociceptive processing during the psychophysical plateau. Our experiment focuses on the question of whether any structures could fall into the second category and our results answer this affirmatively. We have confirmed the observation [21,34] that, during the continuous application of noxious heat to the skin, the perceived intensity of heat pain increases during the first 10-12 s and then remains nearly constant thereafter, a period we have called the *psychophysical plateau*. We have shown further that the activation of cerebral structures changes dramatically during this relatively prolonged cutaneous heating. In particular, both the voxel count and BOLD signal increase in the right MedThal, PosIns, and left S2 cortex

throughout the stimulus duration and during the psychophysical plateau, consistent with the possibility that these structures participate in modulating nociceptive processing during this period. Activity in these structures is not correlated with perceived intensity as measured by COVAS ratings. In contrast, voxel count in the left S1 cortex, and BOLD signal in the bilateral OFC correlated positively only with COVAS ratings and not with stimulus duration; furthermore, the ANOVA analysis showed that the activation of these structures did not change during the psychophysical plateau; these functional relationships are consistent with the participation of these structures in the perception of stimulus intensity.

It is possible that mechanisms operating only at the peripheral, spinal cord, or brainstem levels are alone responsible for the modulation of perceived intensity that forms the psychophysical plateau. However, the participation of active thalamocortical processes cannot be ruled out; this is shown in Figure 6, which depicts the discharge frequency of peripheral and central nociceptive neurons together with the COVAS ratings in our experiment. The neuronal discharge activity presented in Figure 6 is derived from monkeys but the timing of the central neuronal events is not likely to be more than 2 s delayed in humans, given the similarity of the stimulation method and the estimated conduction velocities from the human STT to the cerebral cortex (average 2.9 m/s for C fiber stimulation; averages ranging from ~10 to 21 m/s for Aδ fiber stimulation [28,14,59,69].

As shown in Figure 6, during a prolonged noxious heat stimulus (20-30 s), only type 1 Aδ primate heat nociceptive afferents show increasing activity during the first 10-15 s before reaching a plateau that is maintained throughout the remaining stimulation [72,71]. Other primate heat nociceptive afferents (type 2 Aδ and both rapidly and slowly adapting C fibers) show a decline in activity to a low level within 5-10 s of an initial high level near stimulus onset [44,71]. The initial peak response is followed by a variable decline in discharge frequency, sometimes to very low levels of firing or firing in bursts [13,4,10,35,67]. During this early stimulation period, the discharge of spinothalamic, ventral posterior thalamic, and S1 cortical heat nociceptive neurons increases. Presumably, the increasing COVAS ratings and activity of central neurons during this early period reflects the physiological process of central temporal summation. After peak activity, the firing of spinothalamic and thalamic neurons declines to a lower plateau [32,29]. However, the response profile of most cortical heat nociceptive neurons in the somatosensory (S1) cortex changes dramatically following 10 s of stimulation because there is little if any negative adaptation following the initial peak activity [30,31]. The physiological basis for this difference in thalamic and cortical response profiles has not been established, but the possibility of thalamocortical modulatory mechanisms has been suggested [29].

It is notable that, during the initial 10 s of stimulation, COVAS ratings increase along with increases in spinothalamic, thalamic, and cortical firing frequency while activity in the type 2 Aδ and in both rapidly and slowly adapting C fibers continues decreasing; only the discharge rate of the type 1 Aδ fibers increases (Figure 6). Central temporal summation continues beyond the peaks of spinothalamic, thalamic, and cortical activity as shown by the increasing COVAS rating and its correlation with the BOLD and voxel responses of several cortical areas. Beyond 10 s of stimulation, however, temporal summation appears to be modified because the perceived intensity of heat pain (COVAS) no longer increases despite the continued discharge of spinothalamic, thalamic, and cortical neurons, and increased firing of type 1 Aδ heat nociceptive afferents (Figure 6). Despite continued peripheral afferent firing, including increased input from type 1 Aδ fiber activity, spinothalamic and thalamic discharge frequency begins a steady decline from peak levels to sustained activity at much lower levels. In marked contrast, as noted above, the discharge of most cortical neurons continues near peak levels throughout the remaining stimulus period. The modulation of the cortical response profile and COVAS ratings shown here is consistent

with the participation of active thalamocortical mechanisms, as suggested previously [29], and is supported by our observation that the BOLD and voxel response of some thalamic and cortical structures is correlated with stimulus duration but not perceived stimulus intensity. Our experiment thus provides supportive evidence that thalamocortical processes contribute to the perceptual modulation represented by the psychophysical plateau.

Clinical pathology affecting the thalamus and parietal operculum is frequently associated with central pain syndromes [8,7]. There is ample anatomical and physiological evidence to support a modulatory function of the homolateral S2 cortex on pain-related S1 activity [27,22,77,55,15,[1]]; in addition, the homolateral MedThal and PosIns form a reciprocally connected nociceptively-activated circuit that could modulate pain and related affective functions through the OFC *via* well-known anatomical and functional connections [23,48,26,41,42,43,47]. Activity in the thalamus and PosIns has been linked with pain in numerous functional imaging studies [51,1] but their activation has also been associated also with pain modulation and endogenous analgesia [64] [79,78,73]. The thalamus, for example, has an abundance of inhibitory synaptic profiles through which sensory modulation could occur [25]. Indeed, numerous anatomical and physiological studies, ranging from rats to humans, have demonstrated the robust inhibitory functions of the somatosensory thalamus in both nociceptive and non-nociceptive processing [62,45,58,57,[37],[38],[39],[63],[2],[17],[61],46,36,60,[73]]. As suggested by our results, structures activated during pain may participate in some aspects of both pain perception and in the nociceptive modulation that underlies the psychophysical plateau.

We do not know if the pattern of activation changes we have detected would persist for heat stimulation periods of longer duration. It is possible that these changes are transient and that the responses to longer duration heat stimuli would be determined more by peripheral, spinal, or brainstem mechanisms. Our experiment also does not provide any information about brain responses during cold, mechanical, chemical, or other forms of noxious stimulation. Nonetheless, the temporal shift in the brain activation pattern seen in our experiment resembles strongly the temporal dynamic observed in an earlier PET study [11], showing early heat pain brain activations only in the frontal cortex (premotor, perigenual cingulate, lateral prefrontal, and anterior insular cortices) with activations later, after 40 s of repetitive stimulation, only in the ventral posterior and medial thalamus, and the primary sensori-motor, S2, and mid-posterior insular cortices. This activation pattern coincided with increases in pain intensity and unpleasantness. The results of the present investigation are similar in revealing an early and unique heat pain activation of frontal structures (eg: OFC, ACC, AntIns) followed by posterior insular, parietal (inferior parietal, S1, S2) and thalamic activity. Although the duration and pattern (continuous vs. repetitive) of heat stimulation in these two studies is quite different, the similarity of these responses suggests a common dynamic of brain activation, from frontal to parieto-thalamic, that underlies perceptual changes in prolonged but acute heat pain. Some of these activation changes may be related to early pain-related anticipation and anxiety and the recruitment of thalamo-cortical pain modulatory mechanisms [53,24,50,64,[54],[52],3,56,40,[5]].

In summary, our observations support the hypothesis that supraspinal processes are among the determinants of the temporal dynamics of heat pain. The increased activity of specific thalamic and cortical structures as stimulus duration, but not perceived intensity, increases is consistent with the recruitment of a central mechanism that modulates the activation of pain-related cortical responses and the temporal summation of heat pain.

SUMMARY

We used fMRI to show that active brain mechanisms could contribute to the modulation of the temporal summation of heat pain in healthy humans.

Supplementary Material

Refer to Web version on PubMed Central for supplementary material.

Acknowledgments

Supported by the Dept. of Veteran's Affairs, the Veteran's Educational and Research Association of Michigan, NIH Grant AR46045 (KLC); Bonica (IASP), IBRO and WHO/NINDS Fellowships (TDT), and University of Michigan Medical School SBRP Fellowship (AT). The authors declare no conflict of interest, financial or otherwise, with the content or funding of the research described in this report. The authors thank Susan King for technical support and Dr. Richard Gracely for helpful suggestions on earlier versions of this report.

Reference List

1. Apkarian AV, Bushnell MC, Treede RD, Zubieta JK. Human brain mechanisms of pain perception and regulation in health and disease. Eur J Pain 2005;9:463–484. [PubMed: 15979027]
2. Arcelli P, Frassoni C, Regondi MC, De Biasi S, Spreafico R. GABAergic neurons in mammalian thalamus: A marker of thalamic complexity? Brain Res Bull 1997;42:27–37. [PubMed: 8978932]
3. Bantick SJ, Wise RG, Ploghaus A, Clare S, Smith SM, Tracey I. Imaging how attention modulates pain in humans using functional MRI. Brain 2002;125:310–319. [PubMed: 11844731]
4. Beitel RE, Dubner R. Response of unmyelinated (C) polymodal nociceptors to thermal stimuli applied to monkey's face. J Neurophysiol 1976;39:1160–1175. [PubMed: 825619]
5. Bingel U, Lorenz J, Schoell E, Weiller C, Buchel C. Mechanisms of placebo analgesia: rACC recruitment of a subcortical antinociceptive network. Pain 2006;120:8–15. [PubMed: 16364549]
6. Bingel U, Tracey I. Imaging CNS Modulation of Pain in Humans. Physiology 2008;23:371–380. [PubMed: 19074744]
7. Boivie, J. Central post-stoke pain. In: Cervero, F.; Jensen, TS., editors. Pain. Vol. Vol. 81. Elsevier; Edinburgh: 2006. p. 715-730.
8. Bowsher D. Pathophysiology of central pain. Pain Forum 1998;7:15–17.
9. Brooks J, Tracey I. From nociception to pain perception: imaging the spinal and supraspinal pathways. J Anat 2005;207:19–33. [PubMed: 16011543]
10. Campbell JN, Meyer RA, LaMotte RH. Sensitization of myelinated nociceptive afferents that innervate monkey hand. J Neurophysiol 1979;42:1669–1679. [PubMed: 115969]
11. Casey KL, Morrow TJ, Lorenz J, Minoshima S. Temporal and spatial dynamics of human forebrain activity during heat pain: analysis by positron emission tomography. J Neurophysiol 2001;85:951–959. [PubMed: 11160525]
12. Casey KL, Zumberg M, Heslep H, Morrow TJ. Afferent modulation of warmth sensation and heat pain in the human hand. Somatosens Motor Res 1993;10:327–337.
13. Croze S, Duclaux R, Kenshalo DR. The thermal sensitivity of the polymodal nociceptors in the monkey. J Physiol 1976;263:539–562. [PubMed: 1018278]
14. Cruccu G, Iannetti GD, Agostino R, Romaniello A, Truini A, Manfredi M. Conduction velocity of the human spinothalamic tract as assessed by laser evoked potentials. Neur Rep 2000;11:3029–3032.
15. Davis KD. The neural circuitry of pain as explored with functional MRI. Neurol Res 2000;22:313–317. [PubMed: 10769826]
16. Defrin R, Ohry A, Blumen N, Urca G. Sensory determinants of thermal pain. Brain 2002;125:501–510. [PubMed: 11872608]

17. Duncan GH, Kupers RC, Marchand S, Villemure JG, Gybels JM, Bushnell MC. Stimulation of human thalamus for pain relief: Possible modulatory circuits revealed by positron emission tomography. J Neurophysiol 1998;80:3326–3330. [PubMed: 9862926]

18. Forman SD, Cohen JD, Fitzgerald M, Eddy WF, Mintun MA, Noll DC. Improved assessment of significant activation in functional magnetic resonance imaging (fMRI): use of a cluster-size threshold. Magn Reson Med 1995;33:636–647. [PubMed: 7596267]

19. Friston KJ, Holmes AP, Poline JB, Grasby PJ, Williams SCR, Frackowiak RSJ, Turner R. Analysis of fMRI Time-Series Revisited. Neuroimage 1995;2:45–53. [PubMed: 9343589]

20. Friston KJ, Jezzard P, Turner R. Analysis of functional MRI time-series. Hum Brain Map 1994;1:153–171.

21. Hardy, JD.; Stolwijk, JAJ.; Hoffman, DS. Pain Following Step Increase in Temperature. In: Kenshalo, DR., Sr., editor. The Skin Senses. C.C Thomas; Springfield: 1968. p. 444-454.

22. Hari R, Karhu J, Hämäläinen M, Knuutila J, Salonen O, Sams M, Vilkman V. Functional organization of the human first and second somatosensory cortices: A neuromagnetic study. Eur J Neurosci 1993;5:724–734. [PubMed: 8261143]

23. Heath CJ, Jones EG. An experimental study of ascending connections from the posterior group of thalamic nuclei in the cat. J Comp Neurol 1971;141:397–426. [PubMed: 4101677]

24. Hsieh JC, Stone-Elander S, Ingvar M. Anticipatory coping of pain expressed in the human anterior cingulate cortex: a positron emission tomography study. Neurosci Lett 1999;262:61–64. [PubMed: 10076873]

25. Jones EG. Thalamic circuitry and thalamocortical synchrony. Phil Trans R Soc Lond B 2002;357:1659–1673. [PubMed: 12626002]

26. Jones EG, Burton H. Cytoarchitecture and somatic sensory connectivity of thalamic nuclei other than the ventrobasal complex. J Comp Neurol 1974;154:395–432. [PubMed: 4132971]

27. Jones EG, Powell TPS. Connexions of the somatic sensory cortex of the Rhesus monkey. Brain 1969;92:477–502. [PubMed: 4979846]

28. Kakigi R, Shibasaki H. Estimation of conduction velocity of the spino-thalamic tract in man. Electroencephalogr Clin Neurophysiol 1991;80:39–45. [PubMed: 1703948]

29. Kenshalo DR Jr. Giesler GJ Jr. Leonard RB, Willis WD. Responses of neurons in primate ventral posterior lateral nucleus to noxious stimuli. J Neurophysiol 1980;43:1594–1614. [PubMed: 7411178]

30. Kenshalo DR Jr. Isensee O. Responses of primate S1 cortical neurons to noxious stimuli. J Neurophysiol 1983;50:1479–1496. [PubMed: 6663338]

31. Kenshalo DR, Iwata K, Sholas M, Thomas DA. Response properties and organization of nociceptive neurons in Area 1 of monkey primary somatosensory cortex. J Neurophysiol 2000;84:719–729. [PubMed: 10938299]

32. Kenshalo DR Jr. Leonard RB, Chung JM, Willis WD. Responses of primate spinothalamic neurons to graded and to repeated noxious heat stimulus. J Neurophysiol 1979;42:1370–1389. [PubMed: 114612]

33. Koyama T, McHaffie JG, Laurienti PJ, Coghill RC. The single-epoch fMRI design: validation of a simplified paradigm for the collection of subjective ratings. Neuroimage 2003;19:976–987. [PubMed: 12880826]

34. Koyama Y, Koyama T, Kroncke AP, Coghill RC. Effects of stimulus duration on heat induced pain: the relationship between real-time and post-stimulus pain ratings. Pain 2004;107:256–266. [PubMed: 14736588]

35. LaMotte RH, Torebjork HE, Robinson CJ, Thalhammer JG. Time-intensity profiles of cutaneous pain in normal and hyperalgesic skin: a comparison with C-fiber nociceptor activities in monkey and human. J Neurophysiol 1984;51:1434–1450. [PubMed: 6737035]

36. Lee JI, Ohara S, Dougherty PM, Lenz FA. Pain and Temperature Encoding in the Human Thalamic Somatic Sensory Nucleus (Ventral caudal): Inhibition-Related Bursting Evoked by Somatic Stimuli. J Neurophysiol 2005;94:1676–1687. [PubMed: 15901758]

37. Lee SM, Friedberg MH, Ebner FF. The role of GABA-mediated inhibition in the rat ventral posterior medial thalamus. I. Assessment of receptive field changes following thalamic reticular nucleus lesions. J Neurophysiol 1994;71:1702–1715. [PubMed: 8064343]

38. Lee SM, Friedberg MH, Ebner FF. The role of GABA-mediated inhibition in the rat ventral posterior medial thalamus. II. Differential effects of $GABA_A$ and $GABA_B$ receptor antagonists on responses of VPM neurons. J Neurophysiol 1994;71:1716–1726. [PubMed: 8064344]
39. Liu XB, Honda CN, Jones EG. Distribution of four types of synapse on physiologically identified relay neurons in the ventral posterior thalamic nucleus of the cat. J Comp Neurol 1995;352:69–91. [PubMed: 7714240]
40. Lorenz J, Minoshima S, Casey KL. Keeping pain out of mind: the role of the dorsolateral prefrontal cortex in pain modulation. Brain 2003;126:1079–1091. [PubMed: 12690048]
41. Mesulam MM, Mufson EJ. Insula of the old world monkey. I. Architectonics in the insulo-orbito-temporal component of the paralimbic brain. J Comp Neurol 1982;212:1–22. [PubMed: 7174905]
42. Mesulam MM, Mufson EJ. Insula of the old world monkey. II. Afferent cortical input and comments on the claustrum. J Comp Neurol 1982;212:23–37. [PubMed: 7174906]
43. Mesulam MM, Mufson EJ. Insula of the old world monkey: III. Efferent cortical input and comments on function. J Comp Neurol 1982;212:38–52. [PubMed: 7174907]
44. Meyer RA, Campbell JN. Evidence for two distinct classes of unmyelinated nociceptive afferents in monkeys. Brain Res 1981;224:149–152. [PubMed: 7284829]
45. Morrow TJ, Casey KL. State-related modulation of thalamic somatosensory responses in the awake monkey. J Neurophysiol 1992;67:305–317. [PubMed: 1569463]
46. Morrow TJ, Casey KL. Attention-related, cross-modality modulation of somatosensory neurons in primate ventrobasal (VB) thalamus. Somatosens Mot Res 2000;17:133–144. [PubMed: 10895884]
47. Mufson EJ, Mesulam MM. Thalamic connections of the insula in the rhesus monkey and comments on the paralimbic connectivity of the medial pulvinar nucleus. J Comp Neurol 1984;227:109–120. [PubMed: 6470205]
48. Nauta WJ. Neural associations of the frontal cortex. Acta Neurobiol Exp 1972;32:125–140.
49. Nielsen FA, Hansen LK. Finding related functional neuroimaging volumes. Art Intell Med 2004;30:141–151.
50. Peyron R, Garcia-Larrea L, Gregoire MC, Costes N, Convers P, Lavenne F, Mauguiere F, Michel D, Laurent B. Haemodynamic brain responses to acute pain in humans: sensory and attentional networks. Brain 1999;122:1765–1780. [PubMed: 10468515]
51. Peyron R, Laurent B, Garcia-Larrea L. Functional imaging of brain responses to pain. A review and meta-analysis (2000). Neurophysiol Clin 2000;30:263–288. [PubMed: 11126640]
52. Ploghaus A, Narain C, Beckmann CF, Clare S, Bantick S, Wise R, Matthews PM, Rawlins JN, Tracey I. Exacerbation of pain by anxiety is associated with activity in a hippocampal network. J Neurosci 2001;21:9896–9903. [PubMed: 11739597]
53. Ploghaus A, Tracey I, Gati JS, Clare S, Menon RS, Matthews PM, Rawlins JNP. Dissociating pain from its anticipation in the human brain. Science 1999;284:1979–1981. [PubMed: 10373114]
54. Ploghaus A, Tracey I, Clare S, Gati JS, Rawlins JN, Matthews PM. Learning about pain: The neural substrate of the prediction error for aversive events. Proc Natl Acad Sci U S A 2000;97:9281–9286. [PubMed: 10908676]
55. Ploner M, Schmitz F, Freund HJ, Schnitzler A. Parallel activation of primary and secondary somatosensory cortices in human pain processing. J Neurophysiol 1999;81:3100–3104. [PubMed: 10368426]
56. Porro CA, Baraldi P, Pagnoni G, Serafini M, Facchin P, Maieron M, Nichelli P. Does Anticipation of Pain Affect Cortical Nociceptive Systems? J Neurosci 2002;22:3206–3214. [PubMed: 11943821]
57. Ralston HJ III, Ralston DD. Medial lemniscal and spinal projections to the macaque thalamus: an electron microscopic study of differing GABAergic circuitry serving thalamic somatosensory mechanisms. J Neurosci 1994;14:2485–2502. [PubMed: 7514207]
58. Roberts WA, Eaton SA, Salt TE. Widely distributed GABA-mediated afferent inhibition processes within the ventrobasal thalamus of rat and their possible relevance to pathological pain states and somatotopic plasticity. Exp Brain Res 1992;89:363–372. [PubMed: 1320573]
59. Rossi P, Serrao M, Amabile G, Parisi L, Pierelli F, Pozzessere G. A simple method for estimating conduction velocity of the spinothalamic tract in healthy humans. Clin Neurophysiol 2000;111:1907–1915. [PubMed: 11068222]

60. Saade NE, Al Amin H, Baki S Abdel, Safieh-Garabedian B, Atweh SF, Jabbur SJ. Transient attenuation of neuropathic manifestations in rats following lesion or reversible block of the lateral thalamic somatosensory nuclei. Exp Neurol 2006;197:157–166. [PubMed: 16214132]
61. Saadé NE, Kafrouni AI, Saab CY, Atweh SF, Jabbur SJ. Chronic thalamotomy increases pain-related behavior in rats. Pain 1999;83:401–409. [PubMed: 10568847]
62. Salt TE. Gamma-aminobutyric acid and afferent inhibition in the cat and rat ventrobasal thalamus. Neurosci 1989;28:17–26.
63. Salt TE, Eaton SA. Modulation of sensory neurone excitatory and inhibitory responses in the ventrobasal thalamus by activation of metabotropic excitatory amino acid receptors. Neuropharmacol 1995;34:1043–1051.
64. Sawamoto N, Honda M, Okada T, Hanakawa T, Kanda M, Fukuyama H, Konishi J, Shibasaki H. Expectation of pain enhances responses to nonpainful somatosensory stimulation in the anterior cingulate cortex and parietal operculum/posterior insula: an event-related functional magnetic resonance imaging study. J Neurosci 2000;20:7438–7445. [PubMed: 11007903]
65. Talairach, J.; Tournoux, A. A Coplanar Stereotaxic Atlas of the Human Brain. Thieme Medical Publishers, Inc.; New York: 1988.
66. Tillman DB, Treede RD, Meyer RA, Campbell JN. Response of C fibre nociceptors in the anaesthetized monkey to heat stimuli: correlation with pain threshold in humans. J Physiol 1995;485:767–774. [PubMed: 7562615]
67. Tillman, DB. Thesis Dissertation. The Johns Hopkins University; 1992. Heat Response Properties of Unmyelinated Nociceptors; p. 1-187.
68. Tracey I, Iannetti GD. Brainstem functional imaging in humans. Clin Neurophysiol Suppl 2006;58:52–67.
69. Tran TD, Inui K, Hoshiyama M, Lam K, Kakigi R. Conduction velocity of the spinothalamic tract following CO2 laser stimulation of C-fibers in humans. Pain 2002;95:125–131. [PubMed: 11790475]
70. Treede RD, Apkarian AV, Bromm B, Greenspan JD, Lenz FA. Cortical representation of pain: functional characterization of nociceptive areas near the lateral sulcus. Pain 2000;87:113–119. [PubMed: 10924804]
71. Treede RD, Meyer RA, Campbell JN. Myelinated mechanically insensitive afferents from monkey hairy skin: heat-response properties. J Neurophysiol 1998;80:1082–1093. [PubMed: 9744923]
72. Treede RD, Meyer RA, Raja SN, Campbell JN. Evidence for two different heat transduction mechanisms in nociceptive primary afferents innervating monkey skin. J Physiol 1995;483:747–758. [PubMed: 7776255]
73. Wager TD, Scott DJ, Zubieta JK. Placebo effects on human mu-opioid activity during pain. Proc Natl Acad Sci USA 2007;104:11056–11061. [PubMed: 17578917]
74. Woods RP, Mazziotta JC, Cherry SR, Woods RP, Mazziotta JC, Cherry SR. MRI-PET registration with automated algorithm. J Comput Assist Tomogr 1993;17:536–546. [PubMed: 8331222]
75. Woolrich MW, Ripley BD, Brady M, Smith SM. Temporal Autocorrelation in Univariate Linear Modeling of FMRI Data. Neuroimage 2001;14:1370–1386. [PubMed: 11707093]
76. Worsley KJ, Evans AC, Marrett S, Neelin P. A three-dimensional statistical analysis for CBF activation studies in human brain. J Cereb Blood Flow Metab 1992;12:900–918. [PubMed: 1400644]
77. Zhang HQ, Murray GM, Turman AB, Mackie PD, Coleman GT, Rowe MJ. Parallel processing in cerebral cortex of the marmoset monkey: effect of reversible SI inactivation on tactile responses in SII. J Neurophysiol 1996;76:3633–3655. [PubMed: 8985863]
78. Zubieta JK, Bueller JA, Jackson LR, Scott DJ, Xu Y, Koeppe RA, Nichols TE, Stohler CS. Placebo Effects Mediated by Endogenous Opioid Activity on mu-Opioid Receptors. J Neurosci 2005;25:7754–7762. [PubMed: 16120776]
79. Zubieta JK, Smith YR, Bueller JA, Xu Y, Kilbourn MR, Jewett DM, Meyer CR, Koeppe RA, Stohler CS. Regional mu opioid receptor regulation of sensory and affective dimensions of pain. Science 2001;293:311–315. [PubMed: 11452128]

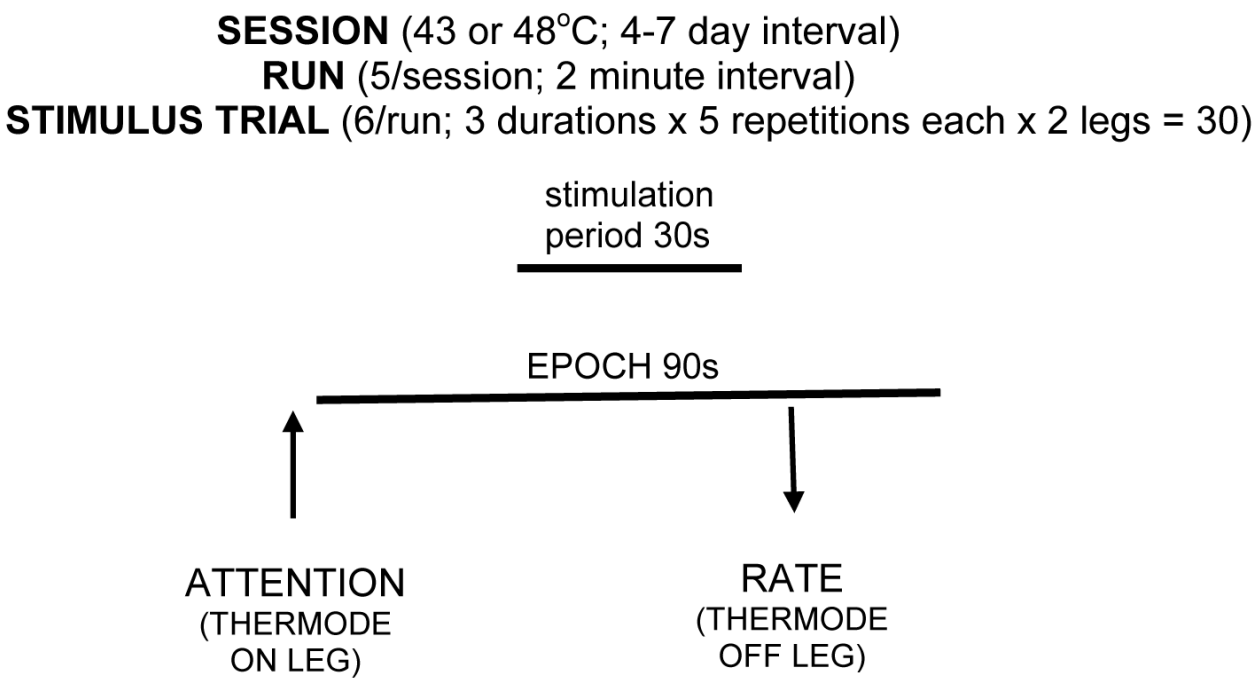

Figure 1.
Summary of data acquisition protocol during the fMRI experiment. The sequence of sessions was counterbalanced among subjects (N = 10). Each stimulus was applied to previously unstimulated skin in each session. Two 30s periods bracketed the 30s stimulation period during each epoch. See text for details.

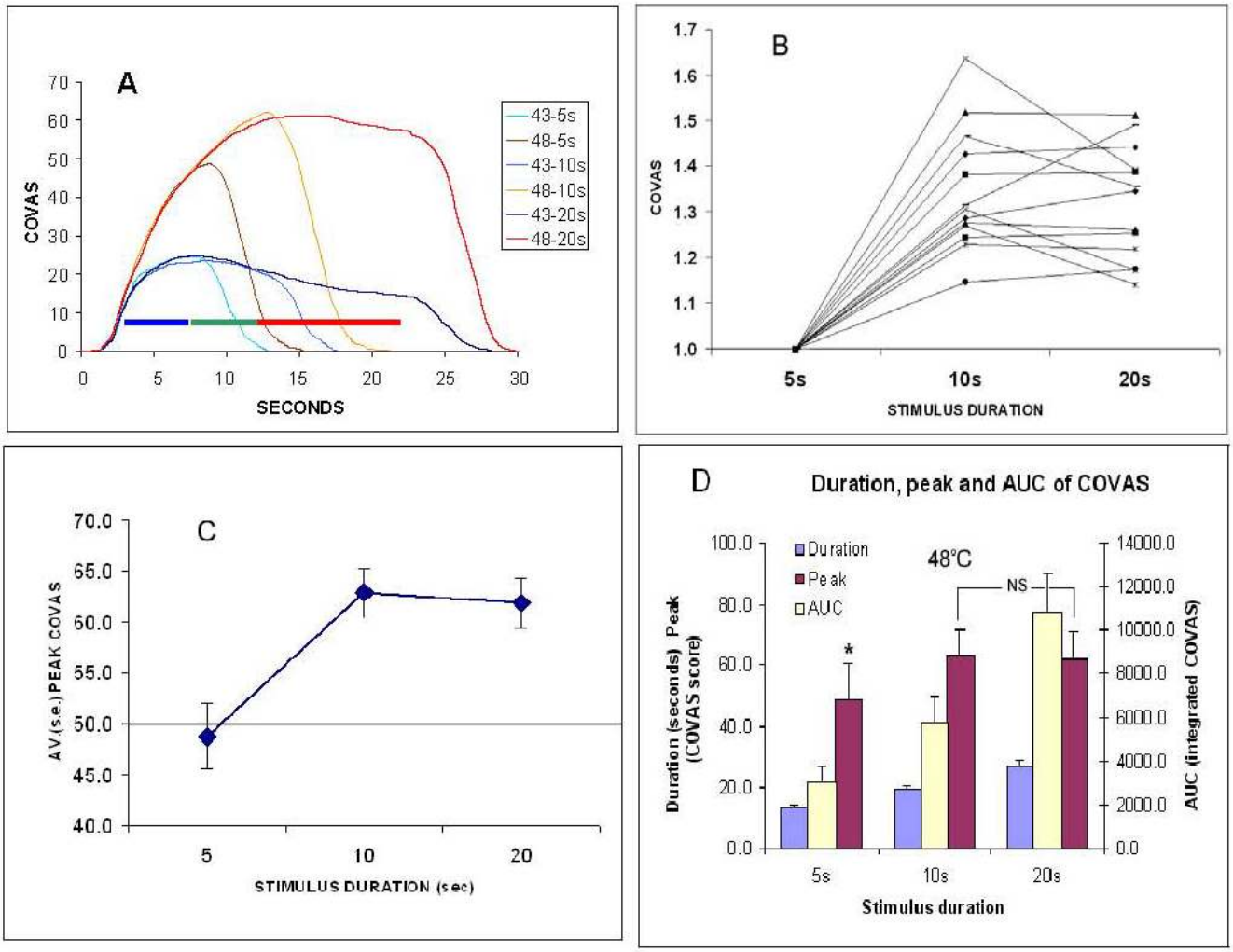

Figure 2.

A. The average COVAS curves of real-time stimulus intensity ratings during the psychophysical experiment. Designated pain threshold is 50. At 43°C (blue curves), the perceived sensation is warm and never painful regardless of stimulus duration. At 48°C, the perceived sensation is increasingly painful when the stimulus duration is extended from 5 to 10s (thin orange and red curves). However, as the duration increases beyond 10 to 20s, the peak perceived intensity does not increase further but remains nearly constant throughout the remainder of the 20s stimulus (thick red curve). The time of the stimulus plateau at 48°C begins ~ 2.5s after stimulus onset and is shown for the 5 (blue bar), 10 (blue + green bars), and 20 s (blue + green + red bars) duration stimuli. B. Normalized (to the rating of 5s duration stimuli) individual peak COVAS ratings of 48°C stimuli of each of the 14 subjects participating in the psychophysical experiment. C. Mean and SE of peak COVAS ratings of 48°C stimulation of all subjects at 5, 10, and 20s duration stimuli in the psychophysical experiment. D. Mean and SD of duration, peak, and area under the curve (AUC) of COVAS curves at 48°C. At 48°C, the COVAS peak of 10s and 20s durations are significantly different from that of the 5s duration stimulus (asterisk; $P < 0.001$); however, the ratings of 10s vs. 20s are not significantly different ($P = 0.413$). At 43°C, the COVAS peaks of 5, 10 and 20s stimulation (not shown) are not significantly different.

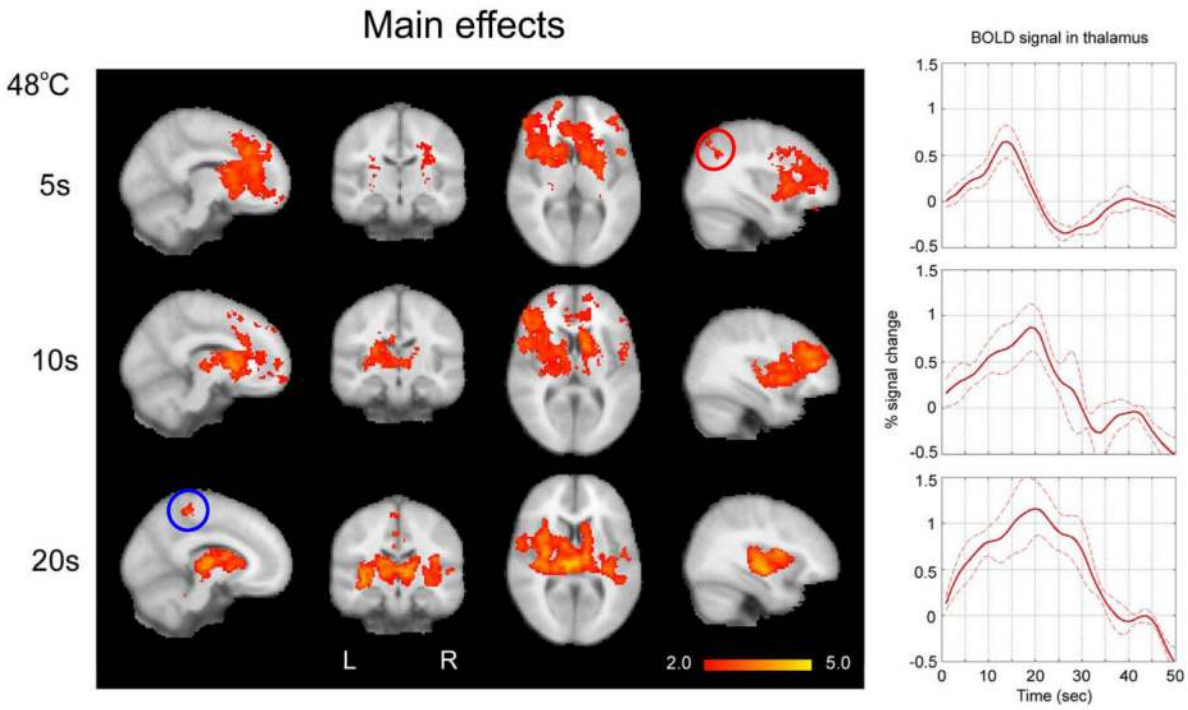

Figure 3.

Activations (Z > 2.0; see color bar at lower right) during increasing durations of noxious contact heat stimulation at 48°C. Images in this and subsequent figures are shown in MNI space. As the stimulus duration increases from 5s to 20s, activations shift from the anterior and pregenual cingulate, anterior insular, orbitofrontal, medial prefrontal, and dorsal lateral prefrontal cortices to the posterior insular cortex and thalamus. In addition, an early activation of the right inferior parietal lobule (red circle; MNI coordinates: 54, −44, 40) is replaced by late activation of the leg area of S1 cortex (blue circle; MNI coordinates: −8, −38, 58). The time series at right shows the right medial thalamic average (and std.error) BOLD signals increasing in amplitude as stimulus duration increases. Although we used the same hemodynamic response function model to extract BOLD responses from all VOI, thalamic activity did not pass statistical threshold during the 5s stimulation (see Figure S2 in supplementary on-line material).

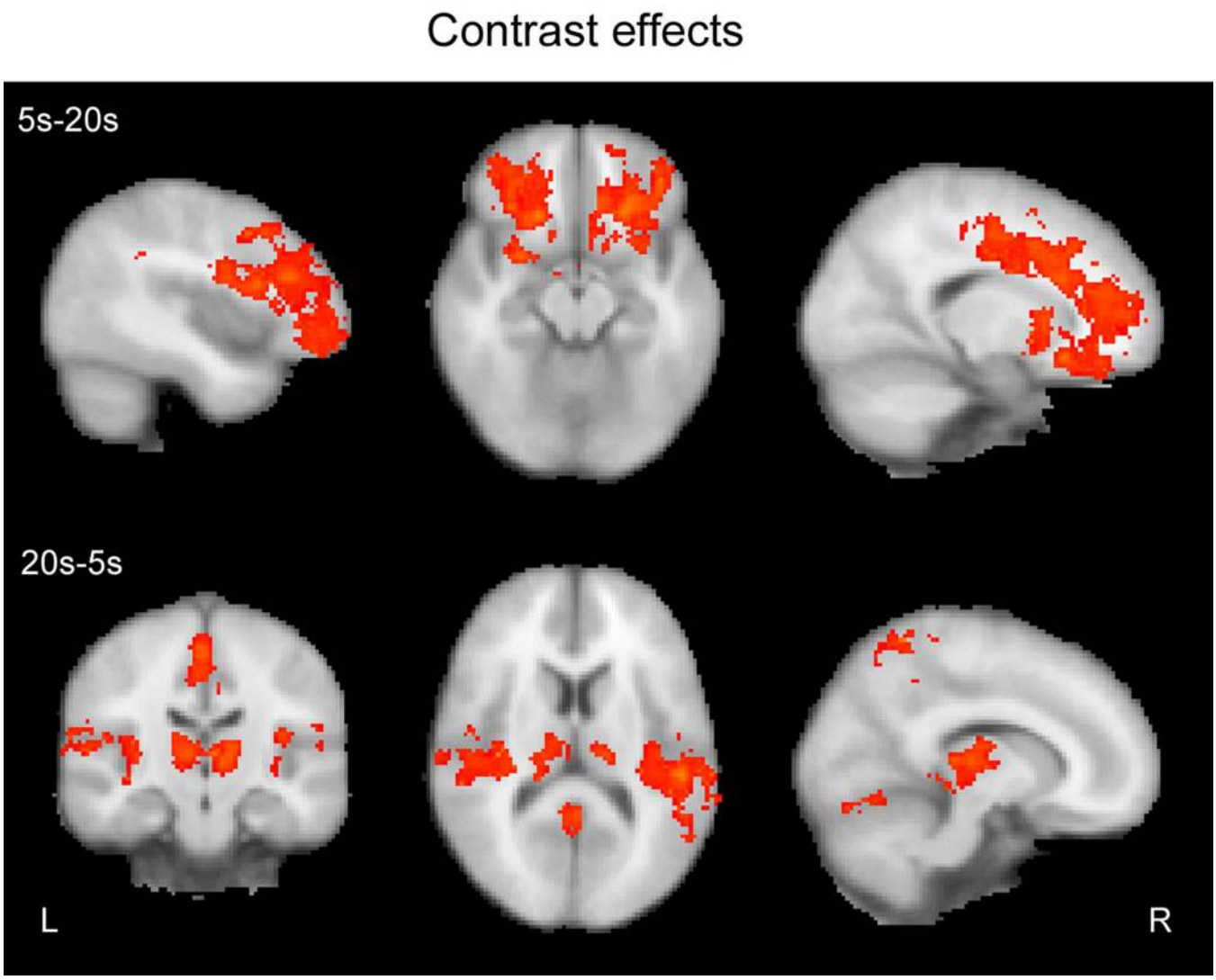

Figure 4.
Activation contrasts (Z > 2.0) during contact heat stimulation at 48°C. Consistent with the main effects, the 5s-20s comparisons (top row) show greater activity in the ACC, OFC and DLPFC of the frontal cortex during the 5s, compared to the 20s stimulus duration. The 20s-5s contrast, however (lower row), shows greater activity in the bilateral posterior insular cortex and thalamic nuclei during the 20s stimulus compared to the 5s stimulus.

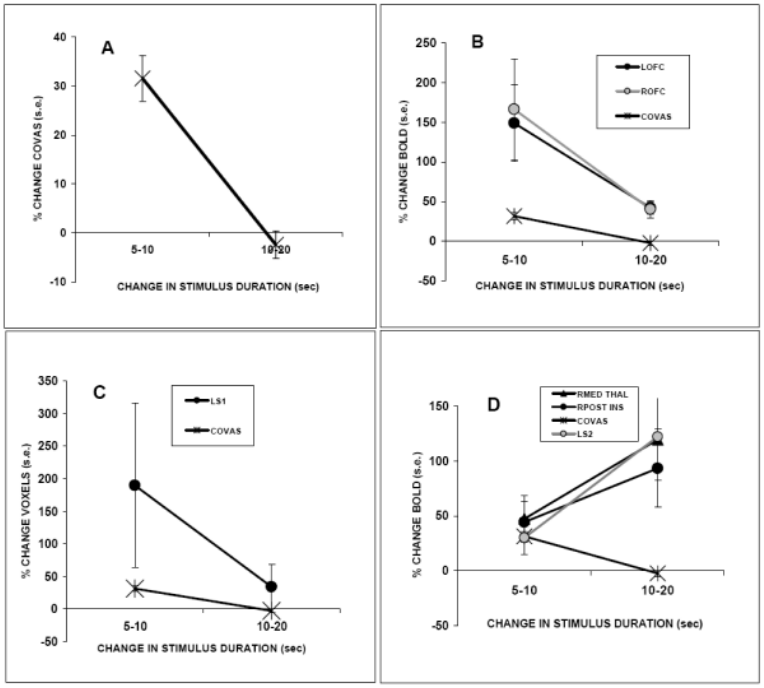

Figure 5.

Average (+/− s.d.) percentage changes in COVAS ratings and in BOLD and voxel counts during changes in stimulus duration from 5s to 10s and from 10s to 20s (during the psychophysical plateau). A. COVAS ratings increase early but show no increase, and even a slight decrease, as stimulus duration increases from 10s to 20s. B. Changes in the peak BOLD signals in the right and left orbitofrontal cortices correlate with the COVAS changes but not with stimulus duration (see Table 2). C. Voxel count changes in the left S1 cortex also correlate with COVAS changes but not with stimulus duration (see Table 2). D. In contrast, both voxel count changes (not shown) and BOLD signal changes in the right medial thalamus, posterior insula, and left S2 cortex correlate with increases in stimulus duration but not with changes in COVAS rating (see Table 2).

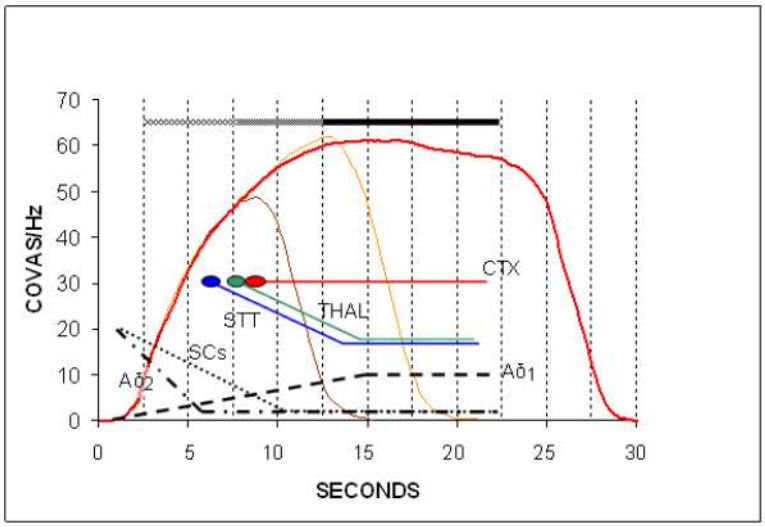

Figure 6.

Diagrammatic representation of the estimated 20 s time courses of neuronal action potential activity during prolonged (~30 s) cutaneous heat stimulation within the noxious range (47-53°C). The frequency of action potentials (Hz) is shown on the same ordinate scale as the real-time COVAS ratings obtained during the psychophysical experiment and shown in Figure 2A. Time courses of the stimulus plateaus in this study are shown above the COVAS curves as increasingly dark bars for the 5, 10, and 20 s duration stimuli (48°C). Peripheral primate nerve fiber activities shown are: dashed line, type 1 Aδ heat nociceptors; dash-dot line, type 2 Aδ and rapidly adapting C heat nociceptors; dotted line, slowly adapting C heat nociceptors (SCs); activity estimates are derived from text and Figure 3 of reference [71] and Figure 2 of reference [44]. The *peaks* of primate central pathway activities (colored ellipses) are shown at equal levels of 30 Hz (arbitrarily chosen for illustrative purposes) followed by the estimated time course of adaptation during the 20 s stimulus. Blue, spinothalamic tract (STT) neurons (activity estimates derived from text and Figure 7 of reference [32]); green, ventral posterior lateral thalamic neurons (THAL) (activity estimates derived from text and Figure 5 of reference [29]); red, primary somatosensory (S1) cortical neurons (CTX) (activity estimate is derived from text and Figures 4 and 5 of reference [30] showing the overall lack of negative adaptation in these neurons *compared* to STT and THAL). Note that, even if accounting for additional activity delays in humans, peripheral afferent activity, with the exception of the type 1 Aδ heat nociceptors, declines before continuing at a lower level during the early stimulation period while COVAS ratings are increasing. Similarly, the activity of spinothalamic and thalamic neurons declines during the 5 and 10 s duration stimulation and during the early phase of the 20 s stimulation before reaching a lower level throughout the remaining stimulation period. Cortical activity, however, declines very slowly or not at all during stimulation [30 , 31] .

Pain. Author manuscript; available in PMC 2011 July 1.

Table 1

A. One-way repeated-measures ANOVA of BOLD signals and voxel counts across durations (5, 10 and 20s)
B. * Post hoc: Bonferroni corrected multiple-paired *t* test (2-tailed)

VOI	BOLD signals		Voxel counts	
	Left	Right	Left	Right
MedTha*	F (2,18) = 13.2, P < 0.001	F (2,18) = 14.3, P < 0.001	F (2,18) = 15.4, P < 0.001	F (2,18) = 21.3, P < 0.001
LatTha*	F (2,18) = 7.4, P < 0.004	F (2,18) = 5.2, P < 0.02	F (2,18) = 15.8, P < 0.001	F (2,18) = 17.1, P < 0.001
PosIns*	F (2,18) = 12.2, P < 0.001	F (2,18) = 9.0, P < 0.002	F (2,18) = 23.3, P < 0.001	F (2,18) = 28.1, P < 0.001
SII*	F (2,18) = 7.0, P = 0.006	NS	F (2,18) = 11.7, P = 0.001	F (2,18) = 6.0, P = 0.01
MidCC*	NS	F (2,18) = 3.8, P = 0.04	F (2,18) = 4.6, P = 0.03	F (2,18) = 12.9, P < 0.001
OFC*	NS	F (2,18) = 11.1, P = 0.001	F (2,18) = 13.0, P < 0.001	F (2,18) = 3.9, P = 0.04
Hipp*	F (2,18) = 8.0, P = 0.003	F (2,18) = 4.3, P = 0.03	NS	NS
PreMot	F (2,18) = 3.6, P = 0.048	NS	NS	NS
InfPar	NS	NS	F (2,18) = 9.5 P = 0.002	NS
SI	NS	NS	NS	F (2,18) = 3.9, P = 0.04
DLPFC	NS	F (2,18) = 4.4, P = 0.03	NS	NS
AntIns	NS	NS	NS	F (2,18) = 7.7, P = 0.004
ACC	NS	NS	NS	F (2,18) = 4.6, P = 0.02
MedPFC	NS	NS	NS	F (2,18) = 3.8, P = 0.042
PregCC	NS	NS	NS	NS
PostCC	NS	NS	NS	NS

	LEFT			RIGHT		
	5s vs. 10s	10s vs. 20s	5s vs. 20s	5s vs. 10s	10s vs. 20s	5s vs. 20s
BOLD signals						
MedTha	t_9 = 2.5, P = 0.03	t_9 = 2.6, P = 0.03	t_9 = 5.3, P < 0.001	NS	t_9 = 4.3, P = 0.002	t_9 = 4.2, P = 0.002
LatTha	NS	NS	t_9 = 4.5, P = 0.02	NS	NS	t_9 = 5.8, P < 0.001
PosIns	t_9 = 2.5, P = 0.03	t_9 = 3.5, P = 0.006	t_9 = 4.1, P = 0.003	t_9 = 2.8, P = 0.02	NS	t_9 = 3.8, P = 0.004
SII	NS	t_9 = 2.7, P = 0.03	t_9 = 2.8, P = 0.02			
MidCC				NS	NS	t_9 = 3.3, P = 0.009
OFC				NS	t_9 = 3.8, P = 0.004	t_9 = 4.6, P = 0.001
Hipp	NS	t_9 = 2.5, P = 0.03	t_9 = 3.4, P = 0.007	NS	NS	t_9 = 2.7, P = 0.02

	LEFT			RIGHT		
	5s vs. 10s	**10s vs. 20s**	**5s vs. 20s**	**5s vs. 10s**	**10s vs. 20s**	**5s vs. 20s**
Voxel counts						
MedTha	NS	$t_9 = 4.0$, P = 0.003	$t_9 = 4.3$, P = 0.002	$t_9 = 2.1$, P = 0.07	$t_9 = 4.5$, P = 0.002	$t_9 = 4.8$, P = 0.001
LatTha	NS	$t_9 = 3.3$, P = 0.009	$t_9 = 5.2$, P = 0.001	$t_9 = 3.5$, P = 0.007	$t_9 = 3.5$, P = 0.007	$t_9 = 4.7$, P = 0.001
PosIns	$t_9 = 3.5$, P =0.007	$t_9 = 3.8$, P = 0.004	$t_9 = 6.1$, P < 0.001	$t_9 = 3.0$, P = 0.02	$t_9 = 4.5$, P = 0.001	$t_9 = 6.7$, P < 0.001
SII	$t_9 = 2.7$, P = 0.03	$t_9 = 3.3$, P = 0.01	$t_9 = 3.8$, P = 0.004	NS	NS	$t_9 = 4.0$, P = 0.0
MidCC	NS	NS	$t_9 = 2.7$, P = 0.03	$t_9 = 2.7$, P = 0.02	$t_9 = 3.5$, P = 0.007	$t_9 = 3.7$, P =0.005
OFC	$t_9 = 3.7$, P =0.005	NS	$t_9 = 4.1$, P = 0.003	NS	NS	$t_9 = 3.4$, P =0.008

Pain. Author manuscript; available in PMC 2011 July 1.

TABLE 2

VOXEL COUNT		**LMedThal**	**LLatThal**	**LPosIns**	***LSII***	**LMidCC**	***LSI***	**LOFC**	**LInfPar**	**Lhipp**			
av. Peak COVAS	Pearson r	0.277	.450(**)	.429(**)	0.339	0.309	.487(**)	−0.055	.500(**)	398(*)			
	Sig. (2-tailed)	0.139	0.013	0.018	0.067	0.097	0.006	0.774	0.005	0.029			
Stimulus Duration	Pearson r	.631(**)	.639(**)	.689(**)	.605(**)	.489(**)	0.271	.445(*)	.639(**)	.378(*)			
	Sig. (2-tailed)	< 0.01	< 0.01	< 0.01	< 0.01	0.006	0.148	0.014	< 0.01	0.04			
		RMedThal	**RLatThal**	***RPosIns***	**RSII**	**RMidCC**							**RACC**
av. Peak COVAS	Pearson r	0.36	0.359	0.361	0.267	0.288							0.145
	Sig. (2-tailed)	0.051	0.051	0.05	0.154	0.123							0.444
Stimulus Duration	Pearson r	.661(**)	.607(**)	.638(**)	.528(**)	.646(**)							.362(*)
	Sig. (2-tailed)	< 0.01	< 0.01	< 0.01	0.003	< 0.01							0.049
BOLD PEAK					***LSII***			***LOFC***			**LPregCC**	**LPostCC**	
av. Peak COVAS	Pearson r				0.355			.449(*)			0.044	−0.364(*)	
	Sig. (2-tailed)				0.054			0.013			0.817	0.048	
Stimulus Duration	Pearsonr r				.500(**)			0.167			.378(*)	0.109	
	Sig. (2-tailed)				0.005			0.378			0.039	0.567	
		RMedThal	**RLatThal**	***RPosIns***				***ROFC***				**RPostCC**	
av. Peak COVAS	Pearson r	0.164	0.065	0.107				.618(**)				−.373(*)	
	Sig. (2-tailed)	0.387	0.734	0.573				0.01				0.042	
Stimulus Duration	Pearsonr r	.477(**)	.402(*)	.456(*)				0.239				0.153	
	Sig. (2-tailed)	0.008	0.028	0.011				0.102				0.419	

Significant at < 0.05

(*)or 0.01

(**)level (2 tailed)